

Selective excitation of Kelvin-Helmholtz modes with rotating electric fields

M. Romé^{1,2}, G. Maero^{1,2}, N. Panzeri^{1,2}, R. Pozzoli¹

¹ *Dipartimento di Fisica, Università degli Studi di Milano, Italy*

² *INFN Sezione di Milano, Italy*

The dynamics of a two-dimensional (2D) inviscid and incompressible fluid can be conveniently studied using a strongly-magnetized pure electron plasma confined in a Penning-Malmberg trap, thanks to a mathematical analogy where the fluid velocity is equivalent to the plasma $\mathbf{E} \times \mathbf{B}$ velocity, and fluid vorticity and stream function correspond to plasma density and electrostatic potential, respectively [1]. Experimental investigations have shed light on dynamical features of the fluid flow ranging from the insurgence and decay of diocotron (Kelvin-Helmholtz) waves to the development of coherent structures and turbulence in conditions of free evolution and more recently also under the effect of an external forcing [2, 3, 4, 5]. Typically, diocotron modes are excited applying multipolar static or oscillating electric fields on an azimuthally-sectorized trap electrode, limiting the maximum mode wavenumber to $N_s/2$, with N_s the number of electrically insulated sectors. A scheme that removes this limit on the accessible wavenumber, based on the application of suitable multipolar rotating electric fields with a drive frequency closely matching the frequency of the desired mode, has been introduced previously [6, 7]. Assuming a stepwise unperturbed radial density profile, $n_0(r) = n_0 H(R_p - r)$, where H denotes the Heaviside step function and R_p is the plasma radius, the equilibrium rotation frequency of the plasma is given by so-called diocotron frequency $\nu_D = e n_0 / 4\pi \epsilon_0 B$, where $-e$ is the electron charge, ϵ_0 the vacuum permittivity and B is the strength of the magnetic field (directed along the symmetry axis of the trap). Here we consider the particular case of a sinusoidally time-varying potentials applied to a 8-sectorized cylindrical electrode with a phase shift of $3\pi/4$ between adjacent sectors,

$$\delta\phi(r = R_w, \theta, t) = \sum_{m=0}^7 V_m(t) [H(\theta - m\pi/4) - H(\theta - (m+1)\pi/4)], \quad (1)$$

where R_w is the radius of the electrode's inner wall, θ denotes the azimuthal angle, and $V_m = V_d \cos(2\pi\nu_d t + \sigma m 3\pi/4)$, with $\sigma = \pm 1$, and V_d and ν_d the amplitude and frequency of the external drive, respectively. Assuming the magnetic field in the positive axial (z) direction, the cases $\sigma = -1$ and $\sigma = +1$ refer to drive electric fields which are “co-” and “counter-”rotating with respect to the azimuthal rotation of the unperturbed plasma, respectively. Using a linear perturbation analysis, it can be shown [7] that a potential on the wall $\delta\phi \propto \exp(i\ell\theta - 2\pi i\nu_d t)$

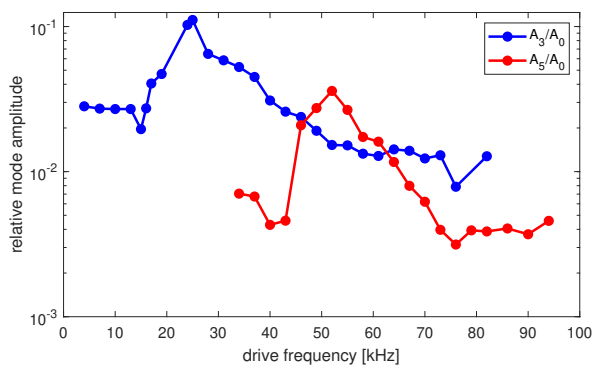


Figure 1: A_l/A_0 of the dominant modes of the plasma cross section deformation *vs* v_d . A drive with $V_d = 2.5$ V is applied for 100 ms.

Figure 2: Plasma density (CCD image) after the application of a co-rotating drive with $v_d = 25$ kHz (see Fig. 1).

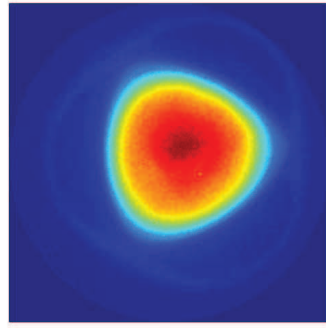
produces a potential perturbation on the plasma surface that is linearly growing with time,

$$\delta\phi(r = R_p, \theta, t) \propto [1 + 2\pi i(lv_D - v_l)t] \exp(il\theta - 2\pi i v_l t), \quad (2)$$

and therefore a significant deformation of the plasma cross section, only when $v_d = v_l = v_D[l - 1 + (R_p/R_w)^{2l}]$, i.e., the frequency of the l -th diocotron mode [8], and $l = 3 + 8k$ for $\sigma = -1$ or $l = 5 + 8k$ for $\sigma = 1$, respectively, with $k = 0, 1, \dots$ an integer index.

The experiments have been performed in the Penning-Malmberg trap ELTRAP [9]. A low density ($n \approx 1.5 \cdot 10^6 \text{ cm}^{-3}$) electron plasma is contained within a stack of cylindrical electrodes (inner radius $R_w = 4.5 \text{ cm}$), kept under ultra-high vacuum conditions (base pressure $\lesssim 10^{-8} \text{ mbar}$). In the experiments reported here, $B = 0.12 \text{ T}$, the plug electrodes are set to a potential of -80 V, and the plasma length is $\approx 90 \text{ cm}$. The electron plasma is generated by applying a radio frequency (RF) drive [10] with amplitude 5.65 V and frequency 7.42 MHz to one of the trap electrodes for 12–15 seconds. The generated plasma has an approximately flat radial density profile, with a mean radius $R_p \approx 0.5R_w$. After switching off the generation drive, the diocotron excitation drive is applied to an 8-sectored electrode for 100 ms, then the plasma is dumped against a positively biased ($V_{ph} = 8 \text{ kV}$) phosphor screen grounding the nearest plug electrode. The light emitted by the phosphor screen is collected by a charge coupled device (CCD) camera, thus obtaining a snapshot of the axially averaged plasma density distribution. The frequency of the drive v_d is varied in successive experimental cycles searching for resonances.

The deformation of the plasma cross section has been chosen as a measure of the mode excitation level. The electron density measured with the CCD camera is fitted on a polar grid with the center of charge of the electron distribution as a reference point. At each radius of the grid, the deviation from the θ -averaged density is Fourier analyzed as $n(r, \theta) - (1/2\pi) \int_0^{2\pi} d\theta n(r, \theta) =$



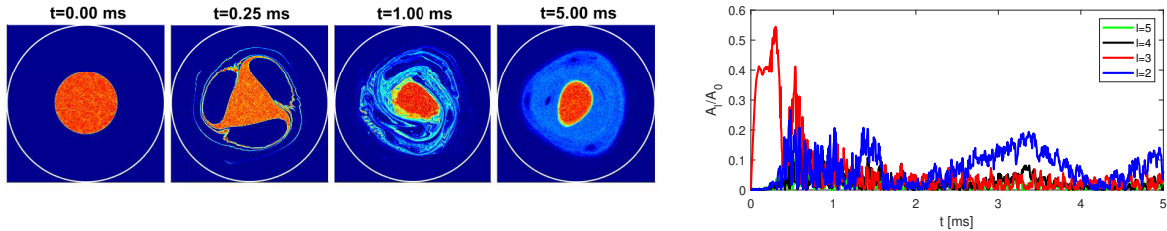


Figure 3: PIC simulation for the case of a co-rotating drive with $V_d = 1.0$ V and $v_d = 33$ kHz.

Figure 4: Time evolution of A_l/A_0 ($l = 2, 3, 4, 5$) for the run of Fig. 3.

$n(r, \theta) - A_0(r) = \sum_{l=1}^{l_{\max}} A_l(r) \sin(l\theta + \varphi_l)$ (with typically $l_{\max} = 10$), and a radially averaged Fourier amplitude is computed as $A_l = (2/R_w^2) \int_0^{R_w} dr r A_l(r)$. These averaged amplitudes A_l normalized over A_0 are shown as a function of v_d in Fig. 1 for $l = 3$ and $l = 5$. The resonance curves appear in general quite broad and the frequencies corresponding to their maxima are shifted with respect to the theoretical values obtained from the idealized case of a stepwise density profile [8]. An example of plasma configuration obtained with the application of a co-rotating drive, showing a well defined triangular plasma cross-section is reported in Fig. 2.

The phenomenon has been also analyzed with a 2D particle-in-cell (PIC) code [11] implementing a guiding-center (fluid) description of the transverse dynamics of the plasma [1]. A Cartesian $N_{grid} \times N_{grid}$ grid is used in the code, and the circular boundary of radius R_w is approximated by a piecewise linear function following the sides of the grid cells. Using a standard bilinear interpolation for the charge density, the Poisson equation for the electrostatic potential is solved by means of a 2D Fast Fourier Transform (FFT) combined with a capacity matrix method. For the time advancement of the electrons a fourth-order Runge-Kutta algorithm is adopted. In the simulations reported here, $B = 0.12$ T, $R_w = 4.5$ cm, $N_{grid} = 256$, and an approximately flat initial density profile is simulated with 10^6 macro-particles randomly distributed within a radius $R_p = 1.8$ cm. The final time of the simulations is 5 ms, and the time step is 10^{-7} s. An example of time evolution, relevant to a co-rotating drive, is reported in Fig. 3. The deformation of the plasma cross section has been estimated using the same kind of analysis performed with the experimental data reported above. The time evolution of A_l for the run of Fig. 3 is shown in Fig. 4. In this example, the evolution of the flow is characterized in the early stage by the a rapid growth of the $l = 3$ mode, which later inversely cascades to an $l = 2$ mode. The stationary state at the end of the simulation is characterized by an elliptically deformed plasma core surrounded by a low-density triangular background arising from the filamentation and mixing of nonlinear structures in the early stage of the evolution. The procedure has been systematically repeated for a number of excitation frequencies around the expected

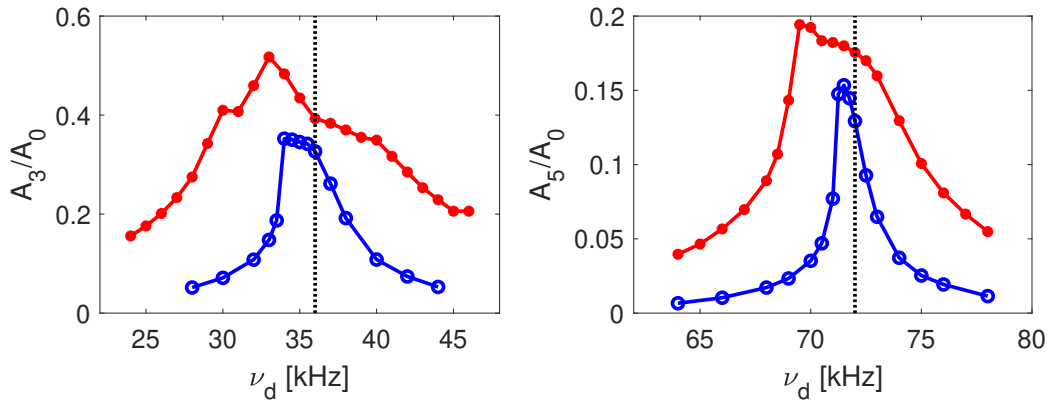


Figure 5: Maximum amplitudes A_l (normalized over A_0) of the dominant modes of the plasma cross section deformation *vs* ν_d obtained from PIC simulations with a co- (left) and a counter- (right) rotating drive, with $V_d = 1.0$ V (red curves) and $V_d = 0.2$ V (blue curves). The dotted lines indicate the resonance frequencies predicted by the linear perturbation theory.

resonance value. The resonance curves relevant to co-rotating and counter-rotating drives for two values of the drive amplitude are reported in Fig. 5. The data correspond to the maximum values achieved by A_l during their time evolution. Similarly to the experiments, the results of the numerical simulations in general confirm the resonant character of the selective diocotron mode excitation. Increasing the drive amplitude, the resonance curves become broader and with down-shifted maxima with respect to the predictions of the linear perturbation theory. Both experiments and numerical simulations will be extended to systematically analyze the presence of unwanted modes depending both on plasma properties like the initial density profile and on the drive amplitude and duration.

References

- [1] M. Romé and F. Lepreti, Eur. Phys. J. Plus **126**, 38 (2011)
- [2] N.C. Hurst, J.R. Danielson, D.H.E. Dubin and C.M. Surko, Phys. Rev. Lett. **117**, 235001 (2016)
- [3] M. Romé, S. Chen and G. Maero, Plasma Phys. Control. Fusion **59**, 014036 (2017)
- [4] S. Chen, G. Maero and M. Romé, J. Plasma Phys. **83**, 705830303 (2017)
- [5] M. Romé, S. Chen and G. Maero, AIP Conf. Proc. **1928**, 020012 (2018)
- [6] G. Bettega, B. Paroli, R. Pozzoli and M. Romé, J. Appl. Phys. **105**, 053303 (2009)
- [7] M. Romé, G. Maero, N. Panzeri and R. Pozzoli, 45th EPS Conf. on Plasma Phys., ECA **42A**, P1.4003 (2018)
- [8] R.C. Davidson, *An Introduction to the Physics of Nonneutral Plasmas* (Addison-Wesley, 1990)
- [9] G. Maero, S. Chen, R. Pozzoli and M. Romé, J. Plasma Phys. **81**, 495810503 (2015)
- [10] B. Paroli, F. De Luca, G. Maero, R. Pozzoli, and M. Romé, Plasma Sources Sci. Technol. **19**, 045013 (2010)
- [11] G. Maero, M. Romé, F. Lepreti and M. Cavenago, Eur. Phys. J. D **68**, 277 (2014)